Multivariable Robust Control of the Plasma Rotational Transform Profile for Advanced Tokamak Scenarios in DIII-D

Wenyu Shi[1], William Wehner[1], Eugenio Schuster[1],
Michael L. Walker[2], David A. Humphreys[2]

[1]Department of Mechanical Engineering and Mechanics, Lehigh University
[2]General Atomics, San Diego, CA

wenyu.shi@lehigh.edu

53rd Annual Meeting of the APS Division of Plasma Physics

This work was supported by the National Science Foundation CAREER Award program ECCS-0645086, and the U.S. Department of Energy under DE-FG02-09ER55064 and DE-FC02-04ER54698.

November 17, 2011

Overview

- System Identification
  - Nonlinear theoreticall plasma models are not suitable for controller design.
  - Data-driven modeling technique is used to obtain a linear dynamic model.
- Feedback Controller Design
  - A mixed-sensitivity robust profile controller is designed to minimize the tracking error and reject external disturbances.
  - An anti-windup compensator is used to keep the profile controller well-behaved in the presence of constraints.
  - The proposed control scheme is tested in the computer simulation.
- Closed-loop Experiments
  - Shot 146419 rejects the large beam disturbances.
  - Shot 146452 & 146462 reject the plasma current disturbances.
  - Experimental results illustrate the performance of the profile controller.

System Identification on DIII-D

- System identification is using mathematical methods to identify linear models of dynamical systems from input/output data.
- The reference plasma state was that of a 1.8 T, β_N-controlled AT scenario, at a normalized pressure $3.5 < \beta_N < 3.9$, and plasma current $I_p = 0.9MA$.
- Actuator modulations were applied from $t = 2.6s$, and the I_p and β_N controls were disabled to ensure no feedback response during data collection.
- The NBI and ECCD systems provided the heating and current drive sources for these experiments.
- Available beam-lines and gyrotrons were grouped to form, together with I_p, five independent H&CD actuators:
  (i) plasma current I_p,
  (ii) co-current NBI power P_{CO},
  (iii) counter-current NBI power P_{CT},
  (iv) balanced NBI power P_{BL},
  (v) total ECCD power from all gyrotrons P_{ECCD}.

System Identification on DIII-D

- The relation between inputs and outputs for any shot can be assumed in the form of

$$\iota(t) = \bar{\iota} + \Delta\iota(t) = \bar{G}(\bar{u}) + P\Delta u(t), \tag{1}$$

  where $\bar{G}$ represents the relationship between the reference feedforward input $\bar{u}$ and reference feedforward output $\bar{\iota}$, $\Delta\iota$ is the feedback output defined as $\Delta\iota = \iota - \bar{\iota}$, and Δu is the feedback input which is defined as $\Delta u = u - \bar{u} = [\Delta I_p \ \Delta P_{CO} \ \Delta P_{CT} \ \Delta P_{BL} \ \Delta P_{ECCD}]^T$ for $u \in \{I_p, P_{CO}, P_{CT}, P_{BL}, P_{ECCD}\}$.
- By subtracting the feedforward value from our data set, we only consider the linear dynamics $\Delta\iota(t) = P\Delta u(t)$. The identified feedback model P can be expressed in the state space form

$$\dot{x}(t) = Ax(t) + B\Delta u(t), \qquad \Delta y(t) = Cx(t) \tag{2}$$

  where the state vector $x(t)$ and output vector $\Delta y(t)$ are defined as $x(t) = \Delta y(t) = \Delta\iota = \iota(t) - \bar{\iota}$, and the C matrix is the identity matrix.
- More details for the system identification can be found from the poster, “Data-Driven Modeling of the Rotation Profile and Magnetic Profile for Advanced Tokamak Scenarios in DIII-D”.

Control System Structure

- A MIMO robust controller based on the linear data-driven model (2) to regulate the evolution of ι will be described. The ι profile control algorithm is summarized by the following steps:

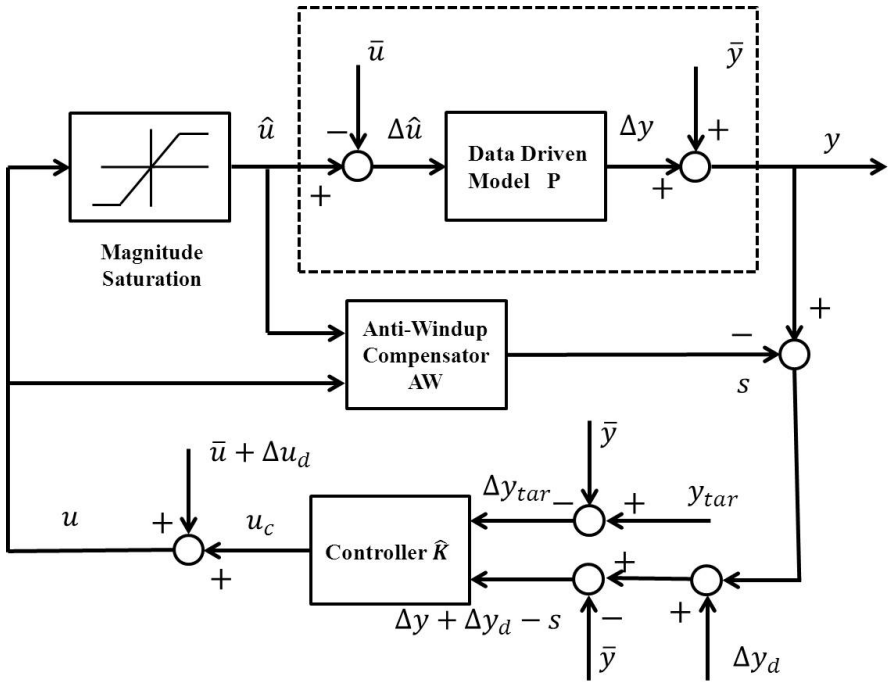

Figure: DIII-D ι-profile control system architecture.

(1) decouple the system and identify the most relevant control channels,
(2) design a H_∞ controller K ignoring control input saturation,
(3) add the anti-windup compensator AW to minimize the adverse effect of any control input saturation.

Design of the Mixed Sensitivity of H_∞ Controller

- Mixed sensitivity is the name given to transfer function shaping problems in which the sensitivity function $M_s = (I + PK)^{-1}$ is shaped along with one or more closed-loop transfer function such as KM_s or $T = I - M_s$.
- H_∞ control is to find a controller stabilizing the closed-loop system while minimizing the maximum singular value of transfer function over all frequencies.
- Based on the output of the singular value decomposition(SVD), the control architecture shown in the following figure is proposed, where two frequency-dependent weighting functions W_p and W_u are introduced.

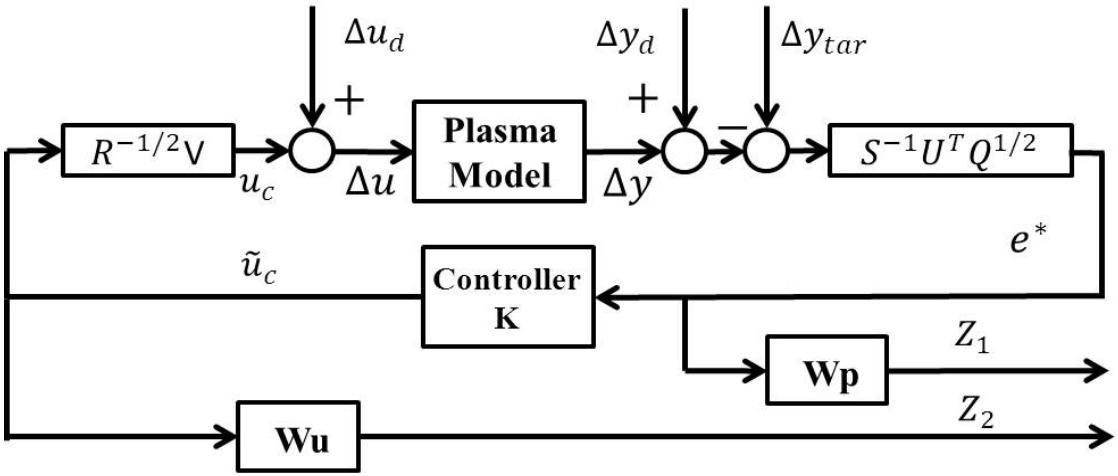

Figure: H_∞ control formulation.

Design of the Mixed Sensitivity of H_∞ Controller

- The feedback system now expressed in the conventional $P^* - K$ robust control framework, is shown in Fig. 3, where P^* is the generalized plant and K is the feedback controller.

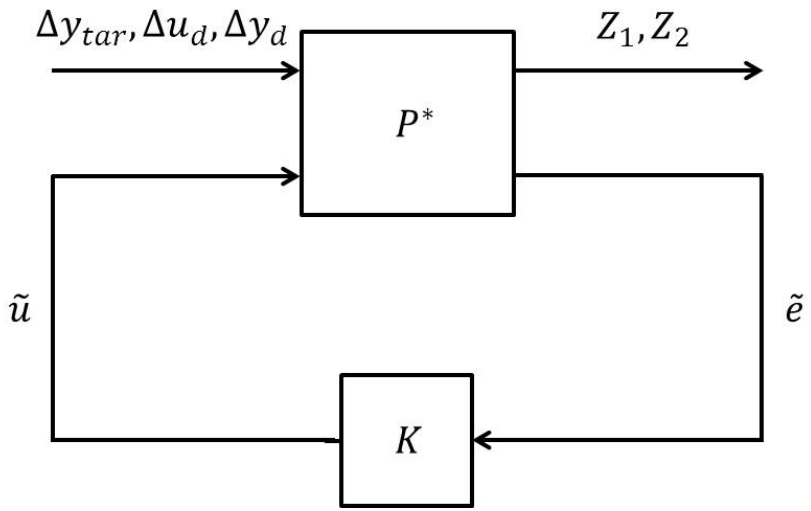

Figure: Model in $P^* - K$ control framework.

- The weighting functions W_p and W_u are parameterized as

$$W_p(s) = K_p\left(\frac{\frac{s}{M_1} + w_{b1}}{s + w_{b1}A_1}\right)^2, \quad W_u(s) = K_u\left(\frac{s + w_{b2}A_2}{\frac{s}{M_2} + w_{b2}}\right)^2$$

where the coefficients M_i, A_i, w_{bi}, for $i = 1, 2$, as well as K_p and K_u, are design parameters in the H_∞ control synthesis.

Design of the Mixed Sensitivity of H_∞ Controller

- We define the transfer function M_s as

$$M_s = (I + S^{-1} U^T Q^{1/2} P R^{-1/2} V K)^{-1}, \tag{3}$$

and write the closed-loop transfer function as

$$T_{zw} = F_l(P^*, K) = \begin{bmatrix} W_p M_s & -W_p M_s P & -W_p M_s \\ W_u K M_s & -W_u K M_s & -W_u K M_s \end{bmatrix} \tag{4}$$

where $F_l(P^*, K)$ is the lower linear fractional transform (LFT).

- We seek a controller $K(s)$ that stabilizes the system and minimizes the H_∞ norm of the transfer function $T_{zw}(P^*, K)$, i.e.,

$$\min_{K(s)} \| T_{zw}(P^*, K) \|_\infty = \min_{K(s)} (\sup_\omega \bar{\sigma}[T_{zw}(P^*, K)(j\omega)])$$

where $\bar{\sigma}$ represents the maximum singular value.

- The overall plasma rotational transform ι profile controller can be written as ($U_c(s)$ denotes the Laplace transform of $u_c(t)$ and $E(s)$ denotes the Laplace transform of $e(t)$)

$$\hat{K}(s) = \frac{U_c(s)}{E(s)} = R^{-1/2} V K(s) S^{-1} U^T Q^{1/2} \tag{5}$$

Design of the Anti-windup Compensator

- At the moment of designing the H_∞ controller, the actuator saturations were not considered. As a result of saturation, the actual plant input may be different from the output of the controller. When this happens, the controller output does not drive the plant and as a result, the states of the controller are wrongly updated, which can cause the behavior of the system to deteriorate dramatically, or even become unstable.
- The generic anti-windup compensator is depicted in Fig. 4.

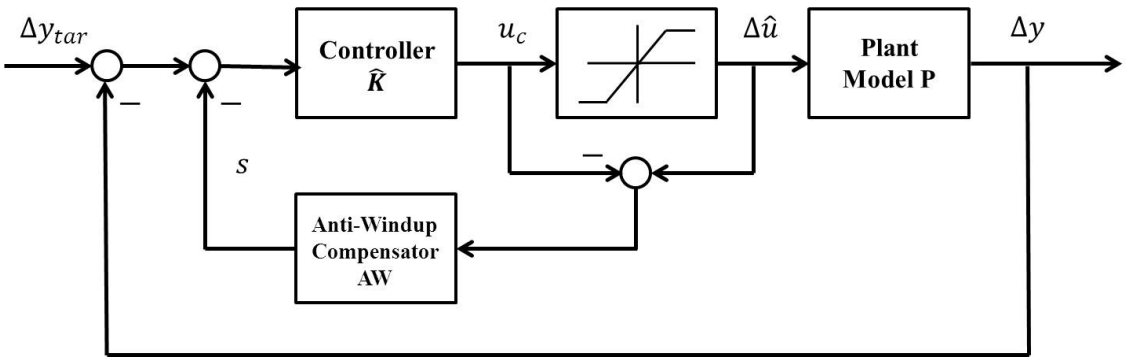

Figure: Scheme of the anti-windup compensator.

- The anti-windup compensator $AW(s)$ adds extra signals to the controller input when control signal saturation occurs. The anti-windup hides the saturation in magnitude from the nominal controller and guarantees in this way that the controller remains well behaved.

Simulated Results

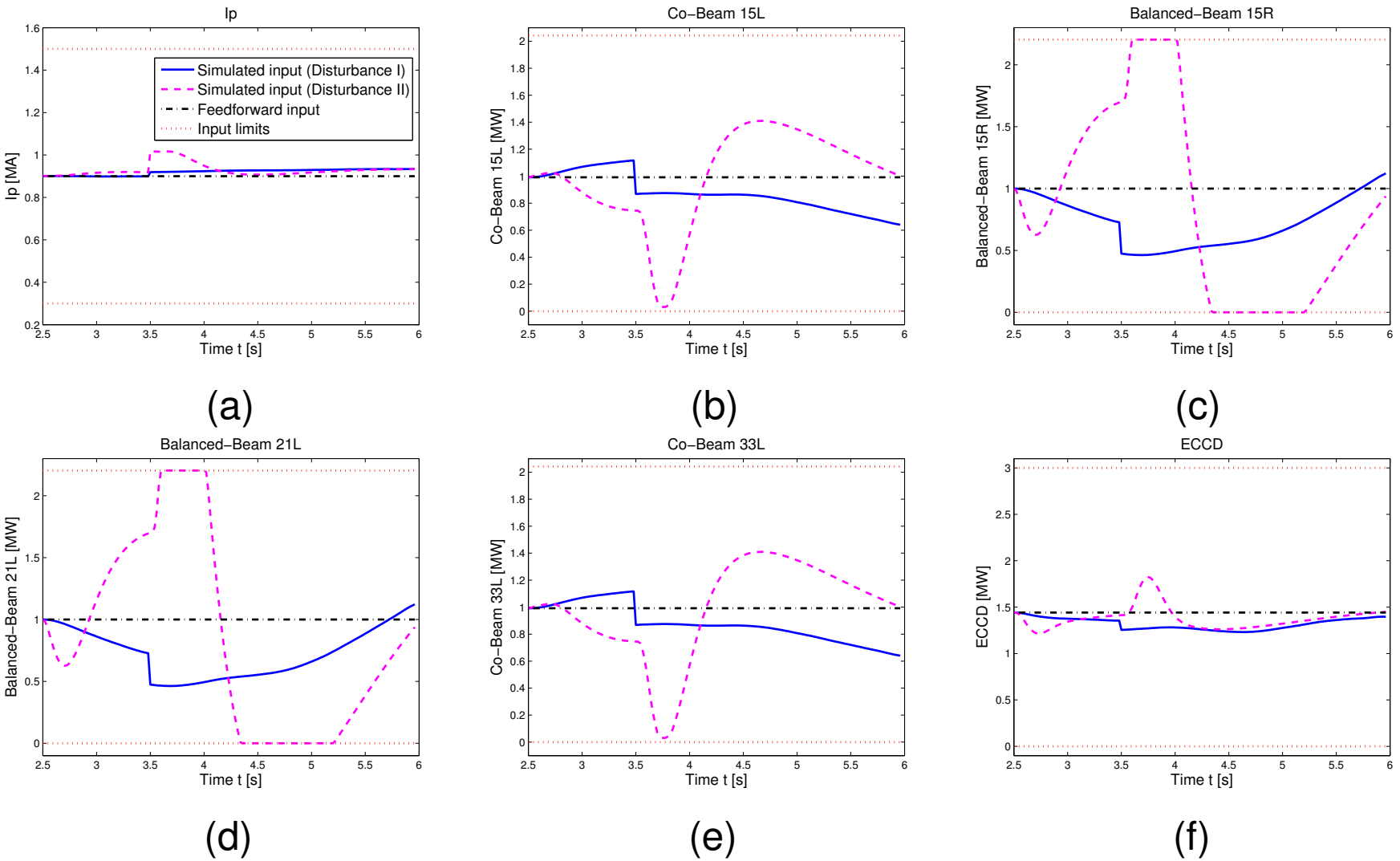

Figure: Simulated control inputs with Disturbance I & II

Simulated Results

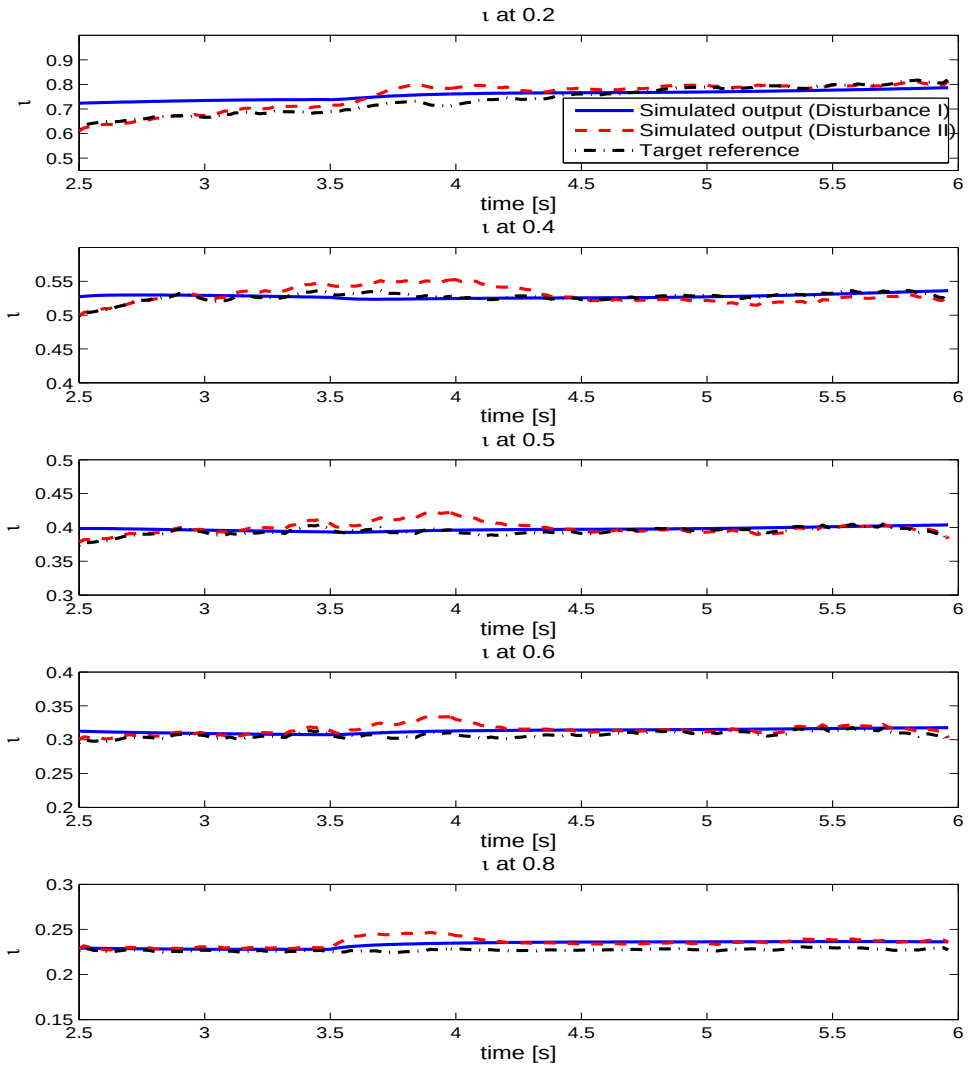

Figure: Simulated ι at $\hat{\rho} = 0.2, 0.4, 0.5, 0.6, 0.8$ with Disturbance I & II

Simulated Results

- In the first second of the simulation, the H_∞ controller effectively regulates ι around the target profile, afterwords the controller tries to reject the input disturbance.
- When large beam disturbances are applied, the beams are not saturated. However, beam values reach saturation very fast when large current disturbance is applied, which activates the anti-windup compensator as shown in Fig. 5 (b)-(e).
- The simulated outputs are shown in Fig. 6. After the disturbance is switched on at 3.5 s, the influence of disturbance especially the Disturbance II is very clear. The robust controller rejects the disturbances and fixes the errors less than one second, and the ι values come back around 4.3 s.

Experimental Results from Shot 146419

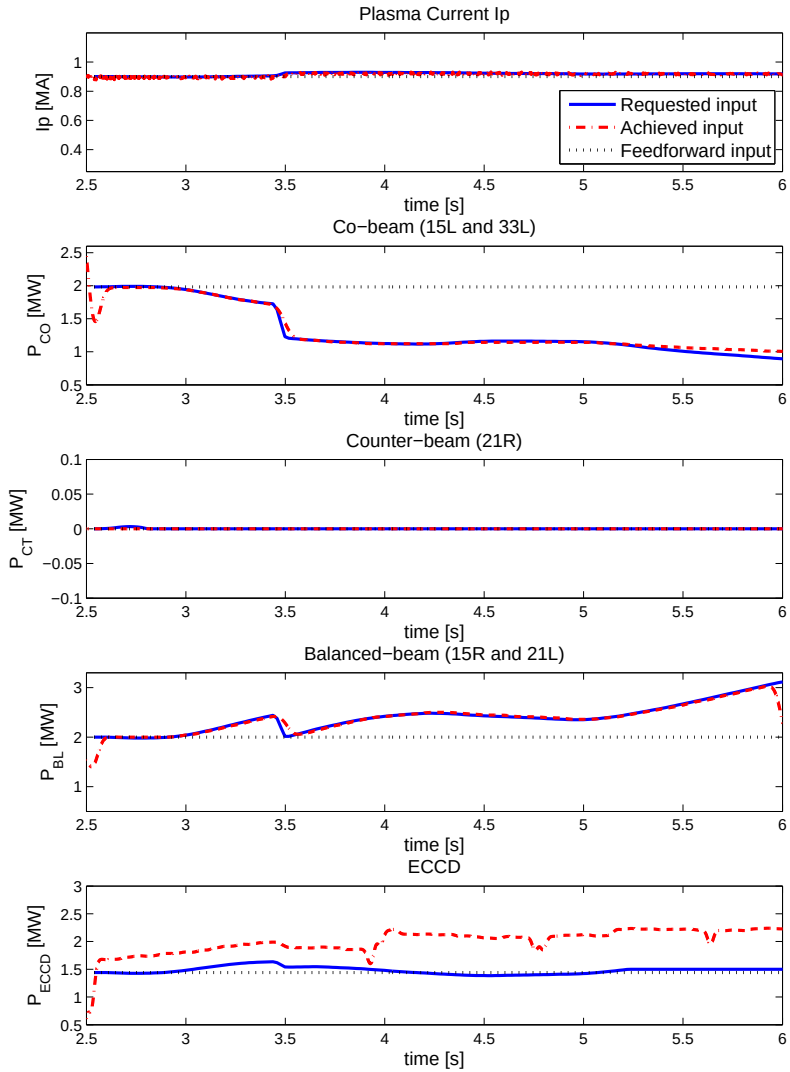

(a)

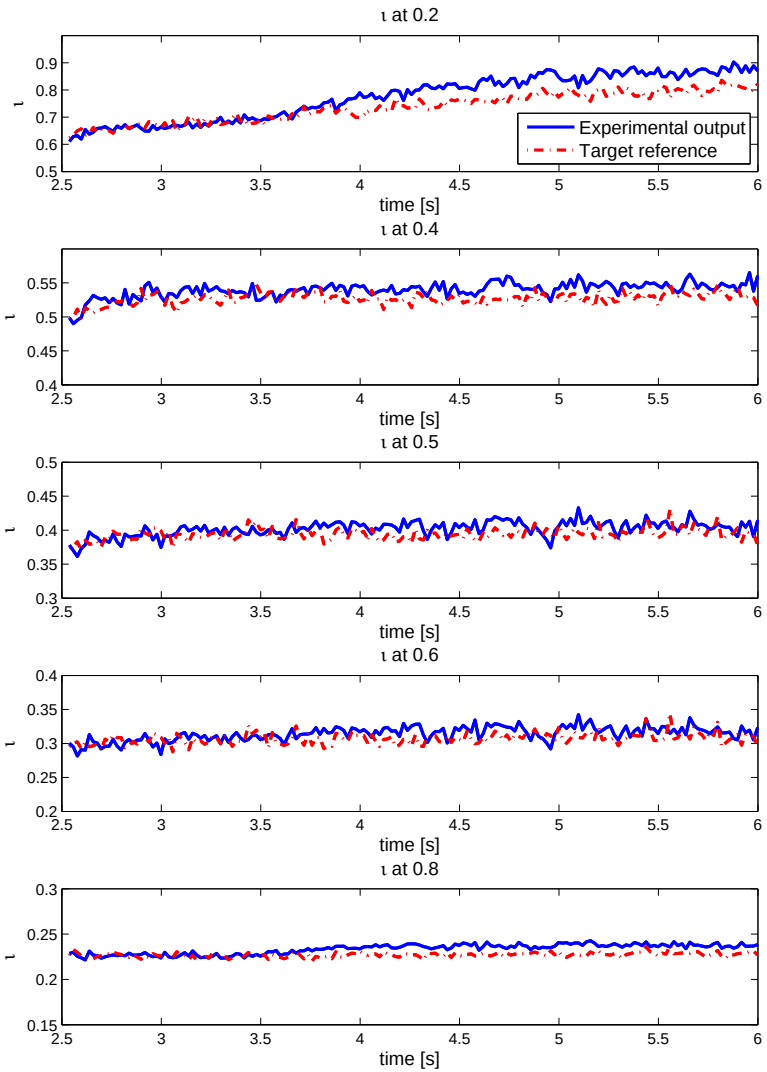

(b)

Figure: (a) Experimental control inputs of shot 146419 (b) Experimental ι profile and target profile at $\hat{\rho} = 0.2, 0.4, 0.5, 0.6, 0.8$ of shot 146419

Experimental Results from Shot 146419

- The trend of all inputs is very similar to the simulated results, which means the data-driven linear model successfully approximates the DIII-D tokamak around the target profile.
- The disturbances were added at the experimental time $t = 3.5$s, and the influence is very clear from Fig. 7(a). Most achieved inputs successfully follow the requested inputs, but the achieved value of P_{ECCD} has some difference from the requested one.
- The experimental outputs are shown in Fig. 7 (b). From $t = 2.5$ s to $t = 3.5$ s, there are no input disturbances, and the tracking errors are less than 1%. The tracking worsens at $t = 3.5$ s because of the disturbances. But the controller approximately drives the system to the target profile after about 1.5 seconds.

Experimental Results from Shot 146452

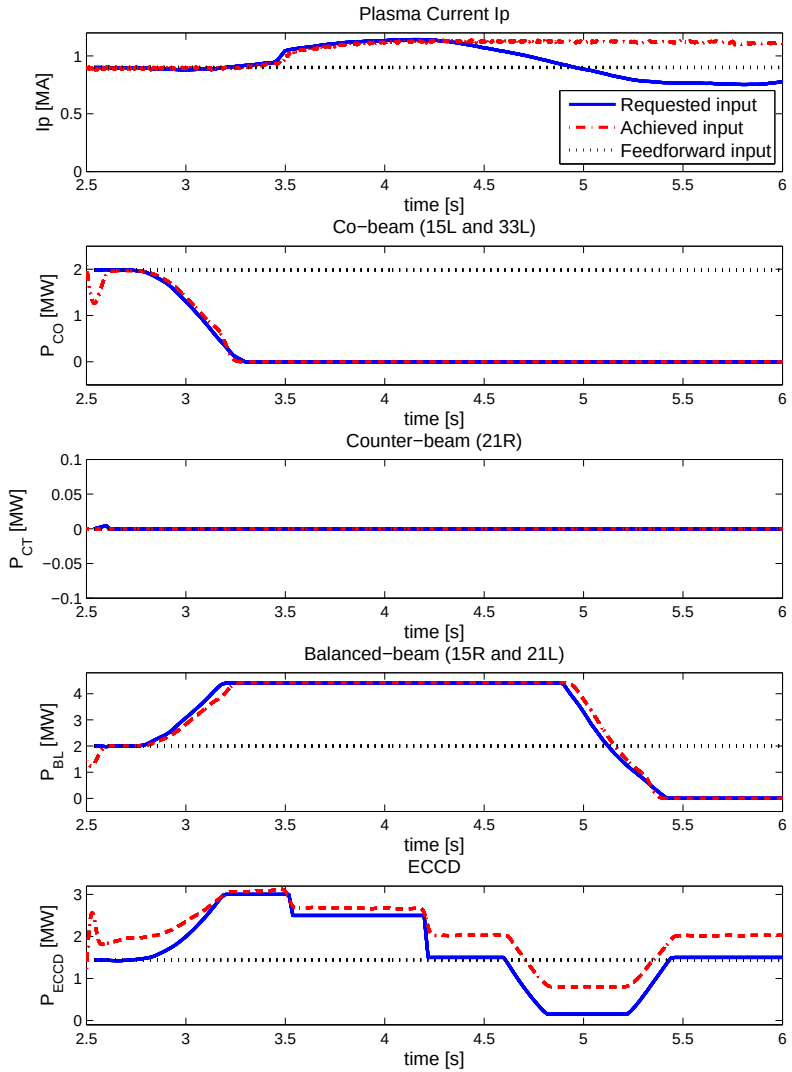

(a)

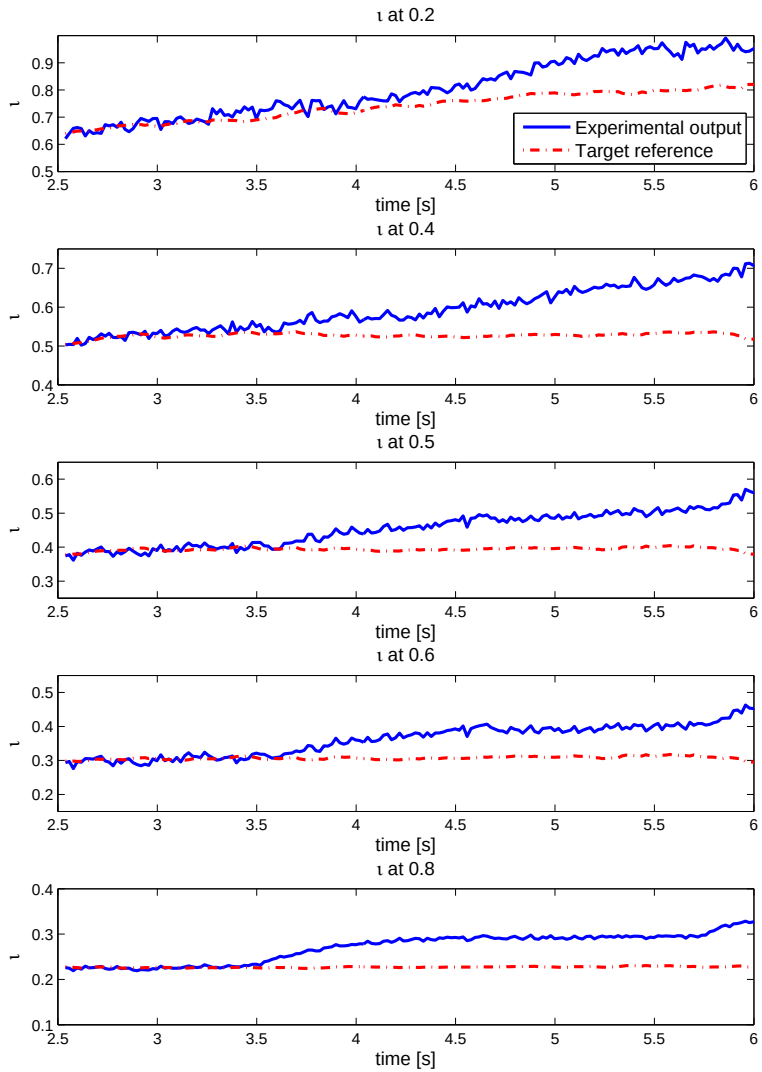

(b)

Figure: (a) Experimental control inputs of shot 146452 (b) Experimental ι profile and target profile at $\hat{\rho} = 0.2, 0.4, 0.5, 0.6, 0.8$ of shot 146452

Experimental Results from Shot 146452

- From $t = 2.5$ s to $t = 3.5$ s, the achieved I_p can follow the requested I_p, but we lose the control of I_p after $t = 4.3$ s. Due to a problem with the setting of the current controller in DIII-D, I_p could only follow requests to increase over time. That is the main reason for failure of control in this shot.
- All beams reach saturation, activating the anti-windup compensator, in an attempt to reduce the profile error, but the beams cannot overcome the error in the achieved I_p.
- The experimental outputs are shown in Fig. 8 (b). From $t = 2.5$ s to $t = 3.5$ s, there are no input disturbances and the achieved I_p follows the requested I_p, resulting in the tracking errors of less than 1%. Because the ι profile is mainly influenced by I_p, after we lose the control of I_p profile control becomes poor.

Experimental Results from Shot 146462

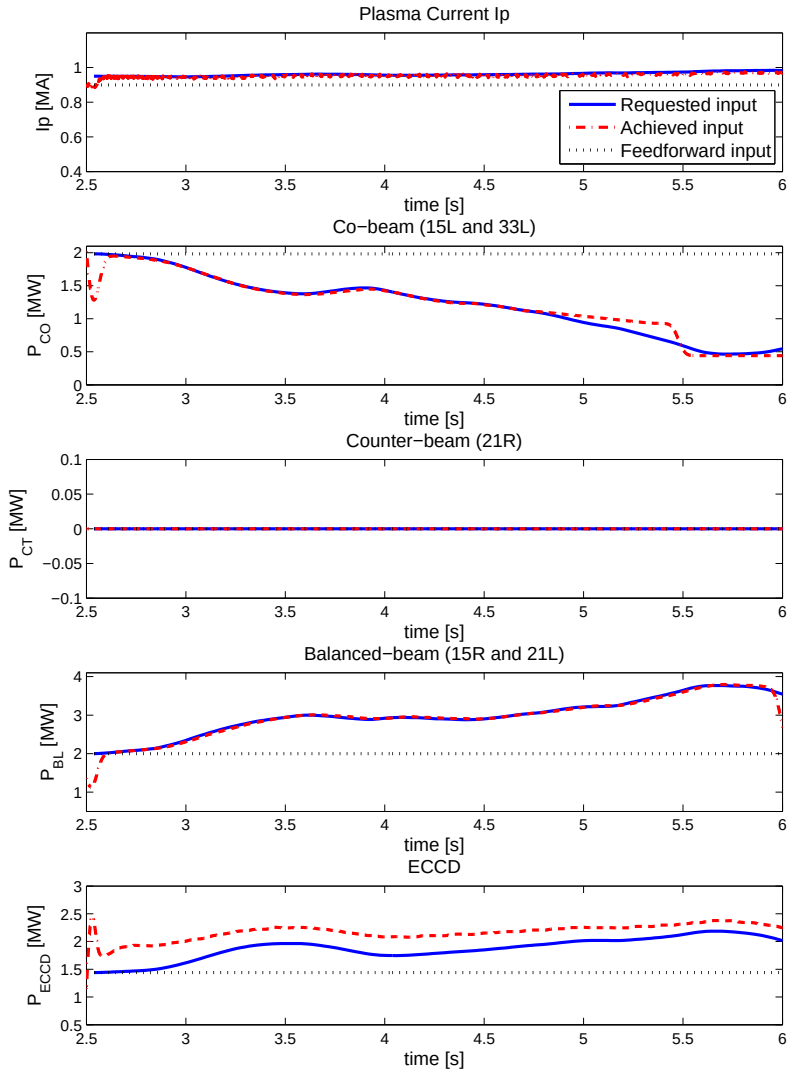

(a)

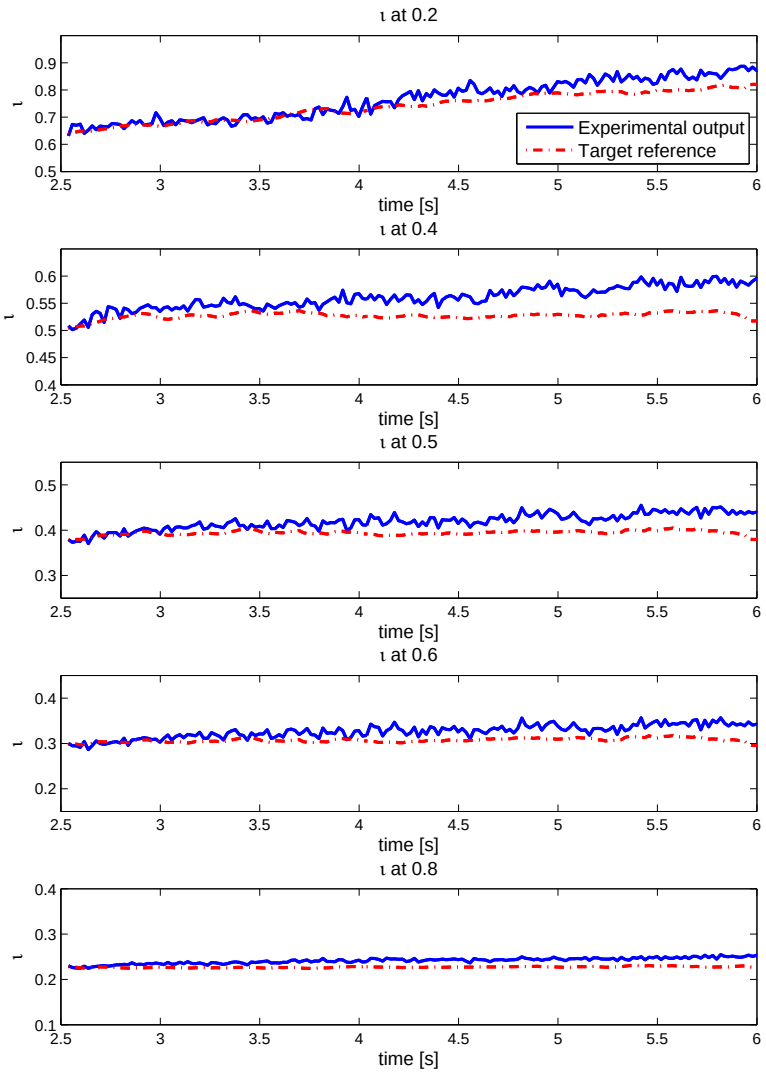

(b)

Figure: (a) Experimental control inputs of shot 146462 (b) Experimental ι profile and target profile at $\hat{\rho} = 0.2, 0.4, 0.5, 0.6, 0.8$ of shot 146462

Experimental Results from Shot 146462

- The requested and achieved experimental inputs are shown in Fig. 9 (a). We see again that the achieved I_p does not follow the requested decrease after $t = 4.75$ s.
- Because the current disturbance $\delta I_p = 0.05$ MA is small, the profile error is small and the beam saturation limits are not reached. Most of the beams successfully follow the requested inputs, but the achieved value of P_{ECCD} has some constant offset from the requested value.
- The experimental outputs are shown in Fig. 9 (b). Because of the small error between requested I_p and achieved I_p after $t = 4.75$ s, there are small tracking errors after $t = 4.75$ s.

Profile Results from All Shots

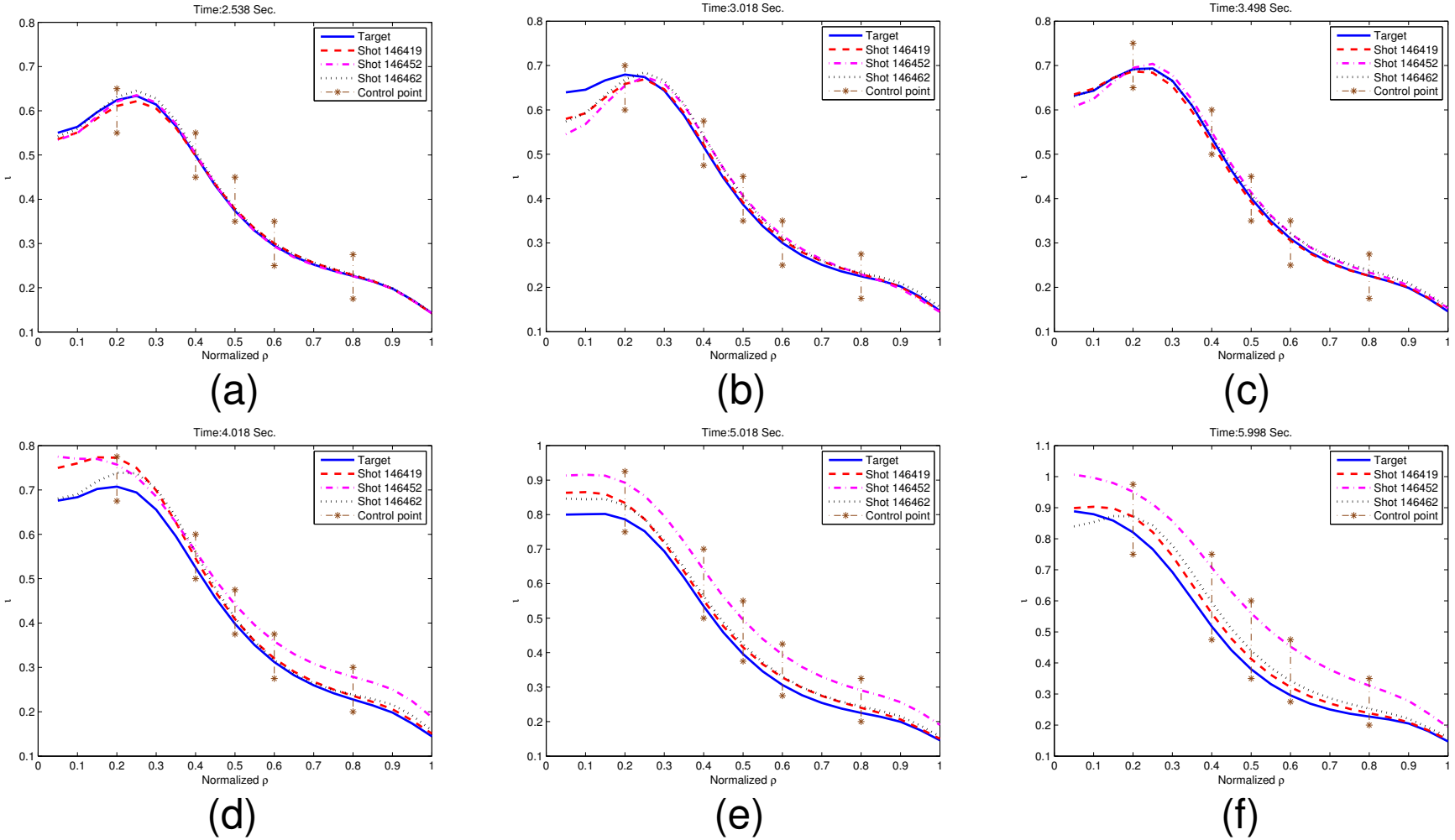

Figure: Plasma $\iota(\hat{\rho})$ profile at time t= 2.538, 3.018, 3.498, 4.018, 5.018, 5.998 seconds from shot # 146419, 146452, and 146462 on DIII-D.

Profile Results from All Shots

- The system identification for the ι profile control was only carried out with 5 Galerkin coefficients computed at normalized coordinate $\rho = 0.2, 0.4, 0.5, 0.6, 0.8$.
- In order to evaluate the ι profile at other points, a series of six plasma ι profiles at different times during the experiments are shown in Fig. 10.
- As can be seen from Fig. 10 (a), (b), (c), the controller is able to keep the ι profile close to the target when there is no external input disturbance for all three shots.
- Fig. 10 (d), (e), (f) show the profiles during the disturbance rejection portion of the shots. As time goes on in shot # 146419 the controller attempts to reject the disturbance, and in shot # 146452 and 146462 the achieved I_p cannot completely follow the request and the results are not well controlled.

Conclusion

- A robust, model-based, MIMO, ι-profile controller was designed for the DIII-D tokamak.
- The mixed sensitivity H_∞ technique is used to minimize the tracking error and optimize input effort ignoring the saturation.
- The anti-windup compensator is applied to minimize the effects of any control input constraint.
- The proposed controller was tested experimentally in DIII-D, and preliminary results show potential for expanding present experimental control capabilities.